Kidney International, Vol. 67 (2005), pp. 2196–2209

Triglyceride accumulation in injured renal tubular cells: Alterations in both synthetic and catabolic pathways

ALI C.M. JOHNSON, ANDREAS STAHL, and RICHARD A. ZAGER

Fred Hutchinson Cancer Research Center, Seattle, Washington; Department of Biochemistry, Stanford University, Palo, Alto, California; and Department of Medicine, University of Washington, Seattle, Washington

Triglyceride accumulation in injured renal tubular cells: Alterations in synthetic and catabolic pathways.

Background. Triglycerides can accumulate in injured tissues, a process thought to represent flux of excess, cytotoxic, free fatty acids into nontoxic triglyceride storage pools. However, this view may be overly simplistic, given that multiple pathways may impact triglyceride levels. This study sought new insights into this issue.

Methods. Cultured human proximal tubule [human kidney-2 (HK-2)] cells or in vivo kidney were subjected to injuries known to increase triglyceride levels ~three- to fourfold [HK-2 cells antimycin A–induced mitochondrial blockade; in vivo glycerol-induced rhabdomyolysis; endotoxemia). Six reverse transcription-polymerase chain reactions (RT-PCRs) were used to monitor mouse/human mRNAs for renal fatty acid transport protein (FATP2), or triglyceride-synthesizing enzymes (acyl-coenzyme A:diacylglycerol acyltransferases DGAT1 and DGAT2). Fatty acid synthase (FAS) and FATP2 were gauged by Western blot. FAS, FATP2, mitochondrial respiration, and phospholipase A2 (PLA_2) effects on cell triglyceride accumulation were probed. Finally, tissue lipase activity was assessed.

Results. Antimycin A up-regulated multiple determinants of HK-2 cell triglyceride formation, including FATP2, FAS, DGAT1, and DGAT2 (proteins and/or mRNAs). However, neither FAS- nor FATP2-inhibition eliminated antimycin A–induced triglyceride loading, indicating the latter's multifactorial basis. PLA_2 activity increased FFA and triglyceride content. Rhabdomyolysis and endotoxemia altered multiple triglyceride homeostatic mechanisms. However, these changes were model-dependent and did not closely parallel those in HK-2 cells. Lipase activity signficantly fell (glycerol) or rose (endotoxemia) with different forms of tissue damage.

Conclusion. Injury-induced triglyceride accumulation stems from multiple, and disease-specific, changes in triglyceride synthetic and degradative pathways. Simple flux of excess FFAs into triglyceride pools is an overly simplistic view of the post-injury-triglyceride loading state.

Key words: triacylglycerol, endotoxemia, rhabdomyolysis.

Received for publication November 15, 2004
and in revised form December 15, 2004
Accepted for publication December 21, 2004

Triglycerides are the body's dominant energy storage form, serving as a depot for, and a source of, free fatty acids (FFAs) for mitochondrial beta oxidation, and hence, adenosine triphosphate (ATP) production [1–3]. In addition, triglyceride formation is thought to represent a cellular cytoprotective response, mitigating so-called "lipotoxicity" (e.g., [4–6]). According to this concept, as injured tissues accumulate excess FFAs from accelerated phospholipase A_2 (PLA_2)–induced phospholipid catabolism, cytotoxicity can result. The latter may arise via a number of mechanisms, including FFA-mediated mitochondrial injury, cytochrome c release [4–6], and direct plasma membrane toxicity or lysis [7–9]. Therefore, shuttling of elevated FFA burdens into triglyceride pools may serve a homeostatic function, staving off FFA-mediated injury, apoptosis, or necrotic cell death [1–3]. Triglycerides are primarily synthesized in liver, intestine, and adipocytes [1]. However, that acyl-coenzyme A:diacylglycerol acyltransferases (DGATs), the enzymes which catalyze the final step of triglyceride synthesis, are expressed in most tissues [10], including kidney [11], suggest the potential broad based relevance of this cytoprotective pathway.

In 1983, Tannenbaum, Purkerson, and Klahr [12] reported that ureteral obstruction causes triglycerides to accumulate in renal cortex and medulla. This study was the first to indicate that renal injury can alter triglyceride metabolism. However, it was not determined whether triglyceride accumulation was unique to obstructive nephropathy [12]. Therefore, this laboratory recently undertook a series of experiments [13] in which triglyceride levels were measured in renal cortex following diverse forms of in vivo renal injury [myoglobinuria, endotoxemia, ischemia/reperfusion (I/R)], and in cell culture experiments [mitochondrial blockade of human kidney-2 (HK-2) cells with antimycin A]. In all instances, three- to fourfold triglyceride increases were observed [13]. The potential pathogenic relevance of this process was suggested by the fact that when proximal tubule (HK-2) cell triglyceride loading was induced by providing excess triglyceride substrate (FFA), altered tubular cell

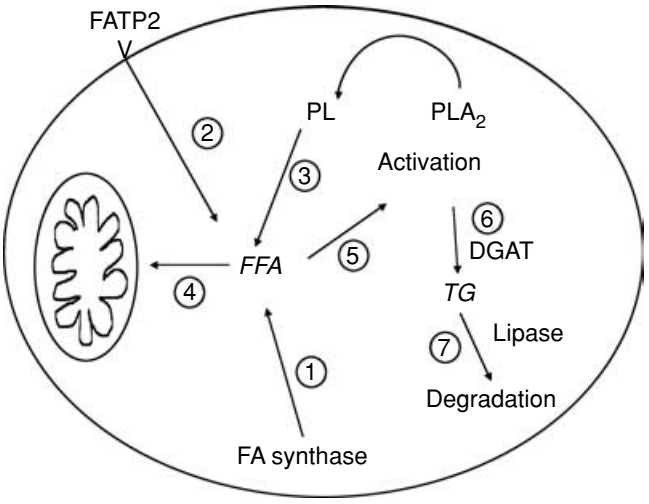

Fig. 1. Schematic of fatty acid homeostasis with triglyceride (TG) incorporation. Free fatty acid (FFA) levels can be supported by (1) in situ synthesis via the action of fatty acid (FA) synthase; (2) intracellular transport via fatty acid transport protein 2 (FATP2), the dominant renal fatty acid transport protein; or (3) injury-induced activation of phospholipase A_2 (PLA_2) with subsequent deacylation of cellular phospholipids (PL). (4) The fatty acids undergo mitochondrial oxidation for adenosine triphosphate (ATP) synthesis. A blockade in mitochondrial respiration, or a reduction in tubular energy demand [e.g., a decrease in glomerular filtration rate (GFR) with a subsequent decrease in tubular sodium reabsorption/ATP consumption], would be expected to decrease mitochondrial fatty acid consumption, and hence, augment the intracellular FFA pool. (5) FFA activation via an ATP-dependent process (forming acyl-coenzyme A) is required for their incorporation into triglycerides. Thus, with severe ATP depletion, a failure of FFA utilization for triglyceride synthesis may result. (6) An increase in activated FFAs would be expected to augment triglyceride formation via DGAT activity. (7) Triglyceride concentrations reflect the balance between triglyceride synthesis and degradation, the latter mediated via lipase activity. Not depicted, potential triglyceride import or export could further alter cellular triglyceride pools. DGAT is the enzyme acyl-coenzyme A:diacylglycerol acyltransferase.

susceptibility to superimposed ATP depletion, or iron-mediated oxidant injury resulted [13].

Cellular triglyceride levels presumably reflect a complex interplay between substrate (most notably FFA) availability, DGAT-mediated triglyceride assembly, and triglyceride catabolism [14–16]. Given these heterogeneous and interactive pathways (schematically depicted in Figure 1 and discussed in its legend), the concept that triglyceride accumulation represents a flux of excess FFAs into triglyceride pools may be overly simplistic. Therefore, the present study was undertaken to gain potential new insights into this issue. Toward this end, extensive studies have been performed in a cell culture model of proximal tubular cell injury. Correlations were then sought with far more complex models of in vivo acute renal failure (ARF) previously noted to evoke a triglyceride loading state [13]. The results of these experiments form the basis of this report.

METHODS

Cultured human proximal tubule (HK-2) cell experiments

General procedures for cell culture experiments. HK-2 cells, an immortalized proximal tubule cell line derived from normal human kidney [17], were used for all in vitro experiments. The cells were maintained in keratinocyte serum-free medium (K-SFM), to which was added 2 mmol/L glutamine, 5 ng/mL epidermal growth factor (EGF), 40 μg/mL bovine pituitary extract, 25 U/mL penicillin, and 25 μg/mL streptomycin, as previously described [17]. All experiments were conducted at near confluence, with cells growing in T75 Costar flasks (Costar, Cambridge, MA, USA). Following specific experiments, as delineated below, cell injury was assessed by% lactate dehydrogenase (LDH) release [8]. Cells were detached from the flasks with a rubber policeman, pelleted by centrifugation, washed ×3 with Hank's balanced salt solution (+ Ca^{2+}/Mg^{2+}) and extracted for either (*1*) lipid (in chloroform:methanol) [13]; (*2*) total RNA (TRIzol method) [18]; or (*3*) protein [18, 19], depending on the specific experiment (see below). Triglyceride values were expressed as nmol/μmol of recovered phospholipid phosphate (Pi) assayed as described elsewhere [20]. RNA samples were used for reverse transcription-polymerase chain reaction (RT-PCR) quantitation of selected mRNA expression [DGAT1, DGAT2, or renal fatty acid transport protein 2 (FATP2) mRNAs, each factored by glyceraldehyde-3-phophate dehydrogenase (GAPDH) signal]. Protein samples were used for Western blot analyses [for FATP2 or fatty acid synthase (FAS); specifics presented below].

Specific HK-2 cell experiments

Antimycin A-mediated triglyceride accumulation: Impact of de novo fatty acid synthesis. This experiment was undertaken to ascertain whether increased fatty acid synthesis is responsible for triglyceride accumulation in response to mitochondrial blockade. T75 flasks of HK-2 cells ($N = 16$) were divided into four groups (four flasks each) as follows: (*1*) control incubation; (*2*) incubation with a FAS inhibitor (cerulenin) [21, 22] (Calbiochem, Santa Cruz, CA, USA) in 0.04% dimethyl sulfoxide (DMSO); (*3*) antimycin A (7.5 μmol/L in 0.1% ethanol); or (*4*) antimycin A + cerulenin. After an 18-hour incubation,% LDH release was determined, and then the cells were subjected to lipid extraction and triglyceride analysis, using an enzymatic assay (#2780-400H) (Thermo Electron, Arlington, TX, USA) [13].

Antimycin A: Effects on FAS expression. To complement the above studies, the impact of antimycin A–mediated mitochondrial blockade on FAS expression was assessed [23, 24]. Eight T75 flasks of HK-2 cells were incubated either with 7.5 μmol/L antimycin A or with its vehicle (0.1% ethanol). After an 18-hour incubation, the

cells were recovered and protein extracts were probed for FAS by Western blotting (described below).

Antimycin A effects on HK-2 cell FATP2 (protein) expression. The following experiment were undertaken to ascertain whether antimycin A causes an increase in the dominant renal tubular plasma membrane fatty acid transport protein, FATP2 [25, 26]. Eighteen flasks of HK-2 cells were incubated for 18 hours either with 7.5 μmol/L antimycin A ($N = 9$) or its vehicle ($N = 9$). The cells were then recovered, protein extracts prepared, and probed for FATP2 (see below).

Antimycin A effects on FATP2 mRNA. Because the above experiment indicated that antimycin A increased FATP2 protein levels (see **Results** section), this experiment ascertained whether that change could be transcriptionally regulated. Sixteen flasks of HK-2 cells were divided into four experimental groups (four flasks each): (*1*) control incubation × 4 hours; (*2*) control incubation × 18 hours; (*3*) 7.5 μmol/L antimycin A treatment × 4 hours; and (*4*) antimycin A treatment × 18 hours. All control incubations were conducted with the antimycinA vehicle (0.1% ethanol). After the incubations, the cells were recovered, the RNA extracted and reverse transcribed (RT), as previously described [18]. FATP2 and GAPDH mRNAs were assessed by multiplexing RT-PCR. The specific methodologies and conditions employed are described below.

DGAT1 and DGAT2 mRNA expression: Effects of antimycin A. To gauge potential effects of antimycin A on DGAT expression, the mRNAs for both DGAT1 and DGAT2 were assessed by RT-PCR, using the same HK-2 cell samples which were probed for FATP2 mRNA (see above). Of note, anti-DGAT antibodies were not available for Western blotting. Hence, these experiments were necessarily restricted to mRNA analyses. The conditions and primers used for DGAT analyses are described below.

PLA_2 effects of HK-2 triglyceride levels. It was previously demonstrated that antimycin A treatment of cultured tubular cells causes PLA_2 induced phospholipid hydrolysis [27]. The following experiment was designed to directly test whether the resulting FFA release results in triglyceride formation. Nine T75 flasks of HK-2 cells were incubated for 3 hours either under control culture conditions ($N = 3$), or with the addition of bovine pancreatic PLA_2 (P8913) (Sigma Chemical Co., St. Louis, MO, USA) (5 or 20 U/mL) [28] ($N = 3$ flasks with each treatment). The cells then underwent lipid extraction and triglyceride enzymatic analysis, as above.

Isolated mouse proximal tubule segment experiments

ARF reduces mitochondrial respiration [decreased sodium reabsorption due to decreased glomerular filtration rate (GFR) and mitochondrial damage/blockade] [29–31]. Therefore, the following experiment was undertaken to ascertain the impact of decreased mitochondrial respiration/blockade on both FFA availability and possible triglyceride formation. To address this issue, experiments were undertaken using freshly isolated mouse proximal tubular segments [32] because they are completely dependent on mitochondrial respiration to sustain ATP levels (unlike HK-2 cells, which can sustain near normal ATP by either aerobic or anaerobic metabolism [33]). Mouse proximal tubules were isolated from two mice as routinely performed in this laboratory [32]. Each preparation was suspended in standard incubation medium [32] and divided into four equal aliquots, as follows: (*1*) control incubation (95% O_2/5% CO_2); (*2*) 5 U/mL of exogenous PLA_2 (as above); (*3*) 100 μmol/L antimycin A; or (*4*) combined antimycin A + PLA_2 treatment. To block antimycin A–induced lethal cell injury, 2 mmol/L glycine was added to each aliquot [34]. After completing 30-minute incubations, lipid extracts were prepared and assayed for FFA [35] and triglyceride content [13]. Values were expressed per mg protein in each tubule aliquot.

In vivo mouse experiments: Glycerol-induced ARF

The following experiments were undertaken to ascertain potential mechanisms by which the glycerol model of ARF induces renal cortical triglyceride loading [13]. Male CD-1 mice (25 to 35 g) (Charles River Laboratories, Wilmington, MA, USA), maintained under normal vivarium conditions, were used for all experiments. On the day of experimentation, the mice were briefly anesthetized with isoflurane and injected with 50% glycerol (total dose of 8.5 mL/kg body weight; administered in equally divided doses into muscle in each hind limb). The mice were allowed to recover from anesthesia, returned to their cages, and provided free food and water access. Eighteen hours later, they were deeply anesthetized with pentobarbital (2 to 4 mg), and the abdominal cavities were opened. One kidney per mouse was resected and saved for subsequent protein, lipid, or RNA extraction, as detailed below. A terminal blood sample was obtained from the inferior vena cava for blood urea nitrogen (BUN) analysis to gauge the severity of ARF. Specific experiments are detailed below:

FATP2: Western blot and mRNA analyses. Seven mice were subjected to the above glycerol model of ARF. Seven sham-injected mice served as controls. Eighteen hours later, a plasma sample was obtained from each mouse for BUN analysis, the kidneys were resected, iced, and the cortices were dissected with a razor blade. The tissues obtained from one kidney per mouse underwent protein extraction for subsequent Western blotting (see below). The cortical tissue from the second kidney was used for RNA extraction for subsequent FATP2 mRNA analysis by RT-PCR (described below).

DGAT1 and DGAT2 mRNA assessments. The above RNA samples, gathered to assess FATP2 mRNA, were also probed for DGAT1 and DGAT2 mRNAs by RT-PCR (see below).

FAS Western blotting. FAS protein expression in kidney at 18 hours post-glycerol treatment was assessed. To this end, four renal cortical protein extracts, obtained 18 hours post-glycerol injection, and four control renal cortical protein extracts, were probed for FAS by Western blot (see below).

In vivo mouse experiments: Endotoxemic ARF

FATP2: Western blot and mRNA analyses. Twenty mice, maintained under routine vivarium conditions with free food and water access, were individually placed in cylindric restrainers and subjected to tail vein injections of 10 mg/kg of purified endotoxin [lipopolysaccharide (LPS) from *Escherichia coli* 0111:B4] (#L-2630) (Sigma Chemical Co.) [13], in 0.1 mL saline. An equal number of control mice received an equal volume of saline containing no LPS. The mice were then returned to their cages. Approximately 18 hours later, the mice were deeply anesthetized with pentobarbital, the abdominal cavities were opened through a midline abdominal incision, and a heparinized blood sample was obtained from the inferior vena cava for BUN analysis. The kidneys were then removed. One was used to prepare a protein extract for subsequent Western blotting for FATP2 (see below). The other was used to extract total RNA for FATP2 mRNA analysis (described below).

DGAT1 and DGAT2 mRNA assessments. Samples of RNA, gathered to assess FATP2 mRNA, were also probed for DGAT1 and DGAT2 mRNAs by RT-PCR ($N = 6$ samples from both control mice and from 18 hours post-LPS–injected mice). The details of those analyses are described below.

FAS Western blotting. Protein samples obtained from five control kidneys and six post-LPS kidneys were probed for FAS. These were analyzed as noted for the post-glycerol samples (see below).

Western blotting methodologies

Renal cortical tissue samples were extracted for protein [36] and probed for either FATP2 or FAS by Western blotting using previously described methodologies [18, 36]. In brief, 10 μg of protein extract (for FATP2) or 150 μg of protein extract (for FAS) were electrophoresed through a 4% to 12% gradient Bis-Tris acrylamide Criterion XT gel (Bio-Rad, Hercules, CA, USA). Proteins were transferred to nitrocellulose membranes using a Hoefer SemiPhor Semi-Dry Transfer apparatus (Amersham-Pharmacia, Piscataway, NJ, USA), according to the manufacturer's instructions. To optimize the transfer of the larger FAS protein (265 kD), conditions were slightly altered, decreasing the addition of methanol to the Tris/glycine buffer (to 10%) and increasing transfer time (2 hours). Membranes were probed for FATP2 with rabbit anti-FATP2 primary antibody at a 1:1500 dilution. The employed rabbit FATP2 antibody preparation was raised (by Andreas Stahl) against the last 26 amino acids of murine FATP2 (MDDAEKTFVPMTENIYNAIIDKTLKL) fused to glutathione-S-transferase (GST) (this antiserum recognized in Western blots a single band of 70 kD solely from kidney and liver lysates, in agreement with the expected tissue distribution and molecular weight of mouse FATP2). FAS was probed with mouse anti-FAS primary antibody (#610963) (BD Transduction Laboratories, San Diego, CA, USA), according to the manufacturer's instructions. Anti-FATP2 and anti-FAS primary antibodies were identified using horseradish peroxidase–labeled donkey antirabbit IgG (#NA-934) (Amersham-Pharmacia), and horseradish peroxidase–labeled sheep antimouse IgG (#NA931) (Amersham-Pharmacia), respectively. Proteins were visualized by enhanced chemiluminescence (ECL Kit) (Amersham-Pharmacia). The relevant protein bands (FATP2, 70 kD and FAS, 265 kD) were semiquantified by densitometry.

HK-2 cells were extracted for proteins and the latter subjected to Western blotting as previously described [18]. FATP2 and FAS detection were performed as noted above (10 μg and 35 μg protein were electrophoresed, respectively).

Nonspecific secondary antibody staining in the above experiments was excluded by the fact that the secondary antibody, in the absence of the primary antibody, did not identify the relevant protein bands. Equal protein loading/transfer was verified by India ink staining. Blot semiquantitative analysis was performed by band densitometry.

Analyses of DGAT1, DGAT2, and FATP2 mRNA by RT-PCR

Mouse. RT-PCR was employed to measure DGAT1, DGAT2, and FATP2 mRNAs in total RNA isolated from mouse renal cortex. Renal cortical tissues, obtained as discussed above, were immediately placed into TRIzol reagent (Invitrogen Life Technologies, Carlsbad, CA, USA). Total RNA was extracted according to the manufacturer's instructions. The final RNA pellet was brought up in RNase-free water to an approximate concentration of 1 to 2 mg/mL.

HK-2 cells. To measure the human homologues of DGAT1, DGAT2, and to assess FATP2 mRNA, total RNA from HK-2 cells was extracted as previously described using TRIzol reagent [18]. The final RNA pellet was brought up in RNase-free water to an approximate concentration of 1 mg/mL.

Table 1. Primers and conditions used for reverse transcription-polymerase chain reaction (RT-PCR) assessments of mouse acyl-coenzyme A:diacylglycerol acyltransferases DGAT1, DGAT2, fatty acid transport membrane 2 (FATP2), and glyceraldehyde-3-phosphate dehydrogenase (GAPDH) mRNAs

Genes	Primer sequences	PCR conditions	Product size
Mouse DGAT1	5′-CTG TGC TCA TGT ATG TCC ACG ACT-3′ 5′-CTG GCT CAT ACC AGT GCT GAG ATT-3′	94°C, 60 sec; 58.5°C, 60 sec; 72°C, 60 sec; 28 cycles	223 bp
Mouse DGAT2	5′-GCA AGA AGT TTC CTG GCA TAA GGC-3′ 5′-GCA GGA CAC ACT AGA AGT GAG CTT-3′	94°C, 60 sec; 58.5°C, 60 sec; 72°C, 60 sec; 24 cycles	833 bp
Mouse FATP2	5′-AGT TCT ACG CAT CCA CTG AAG GCA-3′ 5′-TGA CTG TGG GAT TGA AGC CCT CTT –3′	94°C, 60 sec, 58.5°C, 60 sec; 72°C, 60 sec; 24 cycles	650 bp
Mouse GAPDH	5′-CTG CCA TTT GCA GTG GCA AAG TGG-3′ 5′-TTG TCA TGG ATG ACC TTG GCC AGG-3′	94°C, 60 sec, 58.5°C, 60 sec; 72°C, 60 sec; 18-24 cycles	437 bp

Results, presented in the accompanied figures, are presented as DGAT or FATP2 signals divided by GAPDH signal, as described in text.

Table 2. Primers and conditions used for reverse transcription-polymerase chain reaction (RT-PCR) assessments of human acyl-coenzyme A:diacylglycerol acyltransferases DGAT1, DGAT2, fatty acid transport protein 2 (FATP2) and glyceraldehyde-3-phosphate dehydogenase (GAPDH) mRNAs

Genes	Primer sequences	PCR conditions	Product size
Human DGAT1 homologue	5′-TGC CCG GTT ATT TCT GGA GAA CCT-3′ 5′-AGC TGG GTG AAG AAC AGA ATC TCA-3′	94°C, 60 sec; 59°C, 60 sec; 72°C, 60 sec; 26 cycles	573 bp
Human DGAT2 homologue	5′-TGC TCT ACT TCA CTT GGC TGG TGT-3′ 5′-ACC AGT GGT GAT GGG CTT GGA GTA-3′	94°C, 60 sec; 59°C, 60 sec; 72°C, 60 sec; 26 cycles	701 bp
Human FATP2	5′-TGC TAC TCT TGC CTT GCG GAC TAA -3′ 5′-CCA ATA TTG CCT TCA GTG GCA GCA-3′	94°C, 60 sec; 58°C, 60 sec; 72°C, 60 sec; 30 cycles	261 bp
Human GAPDH	5′-GTC TTC ACC ACC ATG GAG AAG-3′ 5′-GCT TCA CCA CCT TCT TGA TGT CAT C-3′	94°C, 60 sec, 58-59°C, 60 sec; 72°C, 60 sec; 19-25 cycles	490 bp

Results, presented in the accompanied figures, are presented as DGAT or FATP2 signals divided by GAPDH signal, as described in text.

RT-PCR. RT and PCR were performed using the First-Strand Synthesis Kit for RT-PCR (Ambion Inc., Austin, TX, USA) as previously described in detail [19]. The specific primers for mouse and human DGAT1, DGAT2, and FATP2 were designed with 50% to 60% guanine and cytosine (GC) composition (see Tables 1 and 2). The human homologue DGAT1 and DGAT2 sequence products were verified using the Big Dye Terminator Kit (PE-Biosystems, Foster City, CA, USA). The similarity in annealing temperature, but dissimilarity in PCR product sizes, enabled a multiplexing reaction with each set of primers for a given mouse or human message, and the corresponding mouse or human GAPDH (used as a reference housekeeping gene). Each primer set was optimized for a given determination by varying the cycle at which the GAPDH primers were added (mouse GAPDH cycles DGAT1, 18; DGAT2, 19; and FATP2, 24; human GAPDH cycles DGAT1 and DGAT2, 19 and FATP2; 25). PCR products were analyzed by agarose gel electrophoresis and ethidium bromide staining. cDNA bands were visualized and quantified by densitometry using a Typhoon 8600 scanner (Amersham-Pharmacia). DGAT1, DGAT2, and FATP2 cDNA bands were expressed as a ratio to the simultaneously obtained GAPDH cDNA bands.

Tissue lipase assay. The following experiments were undertaken to assess whether renal tubular lipase activity is altered in the aftermath of different forms of injury, potentially impacting triglyceride levels by altering triglyceride hydrolysis. To this end, the following models were employed: (*1*) the glycerol model of ARF in which the renal cortical samples were obtained from 18 mice: nine mice injected with glycerol 18 hours previously and nine control mice; (*2*) the endotoxemic model of ARF in which tissues were collected from 8 mice 18 hours post-tail vein LPS injection, and from eight control mice (18 hours post-sham tail vein LPS injection); and (*3*) I/R injury in which preliminary data indicated that insufficient lipase activity existed in HK-2 cells to allow for accurate assessments using the developed assay (see below); thus, an additional in vivo model of renal injury (I/R) which evokes triglyceride loading [13] was used. Three mice were deeply anesthetized with pentobarbital, a midline laparotomy was performed, the left renal pedicle was identified, and then occluded with a smooth vascular clamp × 15 minutes. Body temperature was maintained at 36 to 37°C with an external heating source. Following vascular clamp removal, the abdominal incisions were sutured and the animals were returned to their cages with free food and water access. Eighteen hours later, the mice were reanesthetized and the post-ischemic left kidneys and the contralateral (control) right kidneys were resected.

Tissue lipase analysis. Renal cortical tissues were dissected and immediately placed into an iced glass dounce homogenizer containing 400 μL potassium phosphate buffer (0.1 mol/L, pH 7.2) with a protease inhibitor cocktail (1 697 498; Roche Diagnostics, Mannheim,

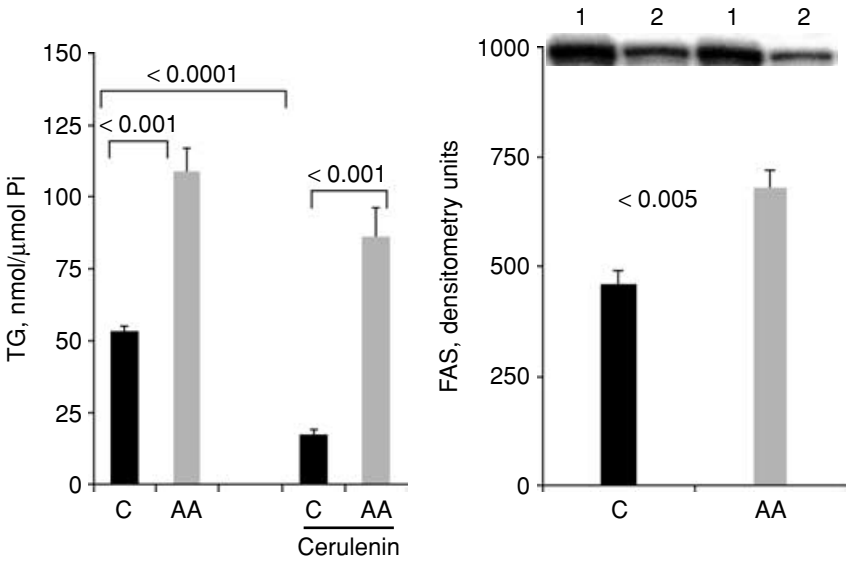

Fig. 2. Fatty acid synthase (FAS): Role in antimycin A (AA)-induced triglyceride (TG) accumulation in human kidney 2 (HK-2) cells. Left panel, HK-2 cells were maintained either under control (C) conditions ± cerulenin; or incubated with antimycin A ± cerulenin (cerulenin used to induce FAS inhibition). Triglyceride levels were assessed 18 hours later. Antimycin A approximately doubled triglycerides, a result which was not blocked by cerulenin. In contrast, cerulenin dramatically reduced triglyceride levels in nonantimycin A–exposed cells ($P < 0.0001$), confirming its ability to inhibit fatty acid synthesis, and hence fatty acid flux into triglyceride pools. Right panel, Antimycin A caused a significant increase in FAS protein, as assessed by Western blot. Representative blots are depicted (lane 1, antimycin A treatment and lane 2, controls).

Germany). The tissues were homogenized on ice with approximately forty strokes, and then the samples were transferred to microcentrifuge tubes. Samples were centrifuged at 14,000 rpm × 15 minutes at 4°C and the supernatants were saved for lipase activity. The tissue extracts (200 μL) were incubated × 2 hours at 37°C with 100 μL of an exogenous triglyceride source (100% canola oil) (Conagra Foods, Irvine, CA, USA). The FFAs which were hydrolyzed from the exogenous triglyceride were measured using the nonesterfied fatty acid colorimetric (NEFA C) kit following the manufacturer's instructions (Wako; Richmond, VA, USA). FFAs were factored by the total protein present in each homogenate sample (bichinoninic protein assay method). The results were expressed as μEq of FFA generated/gram of tissue protein extract. The validity and linearity of the lipase assay was confirmed by a dose-titration curve utilizing exogenous pancreatic lipase (Spectrum Chemicals, Gardena, CA, USA) (0.1 to 25 U/mL) incubated with the canola oil substrate (generated FFAs vs. added lipase concentrations $r = 0.950$).

Calculations and statistics

All values are presented as means ± 1 SEM. Statistical comparisons were made by either unpaired or paired Student t test. Significance was judged by a P value of <0.05. If multiple comparisons were made, the Bonferroni correction was applied.

RESULTS

HK-2 cell experiments

Antimycin A–induced triglyceride accumulation: Impact on fatty acid synthesis and FAS expression.

Triglyceride levels. Antimycin A induced an approximate doubling of HK-2 cell triglyceride content (rising ~60 nmol/μmol Pi over controls) (Fig. 2, left panel). This antimycin A–induced triglyceride increase was not prevented by the presence of cerulenin (triglyceride rising ~70 nmol/μmol Pi, compared to cerulenin treated controls) (Fig. 2, left panel, second two columns). Cerulenin's ability to suppress FAS in HK-2 cells was confirmed by the observation that it decreased triglyceride levels by 70% in nonantimycin A–treated cells (Fig. 2, left panel) ($P <$ 0.0001). In sum, these findings indicate that antimycin A–induced triglyceride accumulation is not dependent on de novo fatty acid synthesis.

LDH release. In the above experiments, antimycin A caused only minimal cell death, as assessed by% LDH release (control cells 8 ± 1% and antimycin A–treated cells 12 ± 1%) ($P < 0.05$). This is consistent with the fact that glycolysis can maintain ~70% of normal HK-2 cell ATP levels in the presence of mitochondrial blockade [33]. Cerulenin had a slight cytotoxic effect (raising LDH release from 8 ± 1% to 12 ± 1%) ($P < 0.05$). However, when present with antimycin A, cerulenin did not increase the extent of antimycin A–induced cell death (12 ± 1%).

Antimycin A effects on HK-2 cell FAS expression. As shown in Figure 2, right panel, antimycin A treatment × 18 hours caused an approximate 33% increase in FAS protein levels, as determined by Western blotting ($P <$ 0.005). Representative blots are depicted (Fig. 2, right panel, lanes 1 and 2 refer to antimycin A–treated cells and control cells, respectively).

FATP2 protein and mRNA expression in response to antimycin A. As shown in Figure 3, left panel, antimycin A treatment ×18 hours produced an approximate 70% increase in HK-2 cell FATP2 protein levels, as assessed by

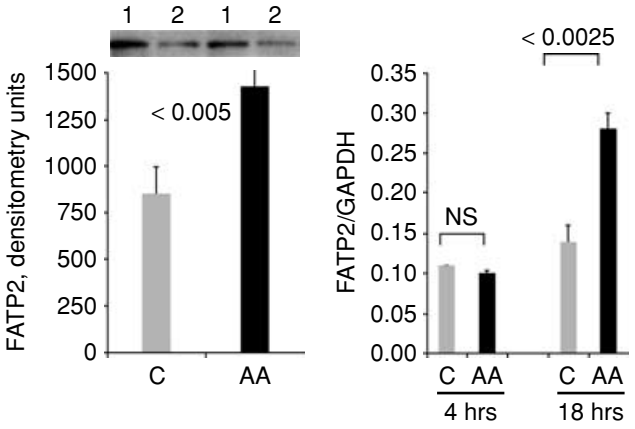

Fig. 3. Antimycin A (AA) effects on fatty acid transport protein 2 (FATP2) protein/FATP2 mRNA expression in human kidney 2 [HK-2] cells. Left panel, Antimycin A treatment caused a significant increase in FATP2 protein, compared to concomitantly incubated control (C) cells. Representative blots are depicted (lane 1, antimycin A and lane 2, control extracts). Right panel, Increased FATP2 mRNA was noted after 18 hours (but not 4 hours) of antimycin A incubation. This temporally corresponded with the increase in FATP2 protein, as noted in the left panel.

Western blot. Representative blots are depicted by their respective bars in the graph (lane 1, antimycin A treatment and lane 2, controls). The FATP2 protein increase corresponded with an approximate doubling of its mRNA (seen at 18 hours, but not at 4 hours post-antimycin A treatment) (Fig. 3, right panel).

DGAT1 and DGAT2 mRNA expression: Effects of antimycin A. DGAT1 message levels ± antimycin A treatment are depicted in Figure 4, left panel. Antimycin A caused a statistically significant increase, seen at both 4-hour and 18-hour time points. As shown in Figure 4, right panel, DGAT2 mRNA was elevated after 4 hours of antimycin A exposure, but with continued (18 hours) antimycin A exposure, it returned to control values.

PLA_2 effects on HK-2 cell triglyceride levels. As shown in Figure 5, left panel, incubating HK-2 cells with either 5 or 20 U/mL of exogenous PLA_2 × 3 hours caused dose-dependent increases in cellular triglyceride levels (consistent with PLA_2-liberated FFAs being channeled into triglyceride). The PLA_2 additions caused dose-dependent, but a quantitatively trivial (<2%), increase in cell death, as assessed by% LDH release (Fig. 5, right panel).

Isolated mouse proximal tubule experiments

FFAs. As shown in Figure 6, left panel, both antimycin A and PLA_2 treatment significantly raised proximal tubule FFA content (controls 9 nmol/mg protein; antimycin A 45 nmol/mg; and PLA_2 31 nmol/mg, respectively) ($P < 0.05$). When PLA_2 and antimycin A were applied together, a profound synergistic FFA increase resulted (to ~250 nmol/mg) ($P < 0.01$).

Triglycerides. As shown in Figure 6, right panel, PLA_2 raised proximal tubular triglyceride content (comparable to the effects seen with PLA_2 treatment of HK-2 cells, as shown in Fig. 5). Despite the fact that antimycin A raised FFAs levels, it caused a 50% reduction in tubule triglyceride content (Fig. 6, right panel). Antimycin A completely blocked PLA_2's ability to raise tubule triglyceride content.

In vivo mouse experiments: Glycerol-induced ARF

FATP2 protein and mRNA analysis.

Protein. At 18 hours post-induction of glycerol-mediated ARF, an approximate 80% reduction in FATP2 protein expression was apparent (Fig. 7, left panel, lane 1, controls and lane 2, glycerol treatment). The glycerol-treated mice had severe rhabdomyolysis-induced ARF, as evidenced by marked elevations in BUN concentrations (post-glycerol 161 ± 7 mg/dL and controls 28 ± 1 mg/dL) ($P < 0.001$).

mRNA. By 18 hours post-glycerol, an approximate 60% suppression in FATP2 mRNA was observed (Fig. 7, right panel). Thus, at the height of the ARF (18 hours post-glycerol injection), and hence, the height of renal cortical triglyceride loading [13], marked reductions in both FATP2 protein and its mRNA were observed.

DGAT1 and DGAT 2 mRNAs post-glycerol injection. DGAT1 and DGAT2 mRNAs at 18 hours post-glycerol injection are depicted in Figure 8, left panel. No change is DGAT1 message was observed. However, there was an approximate two thirds reduction in DGAT2 mRNA, a result which corresponds with a three- to fourfold increase in renal cortical triglyceride levels [13].

FAS protein post-glycerol treatment. Mouse kidney cortex obtained 18 hours post-glycerol injection demonstrated an approximate 50% reduction in FAS expression, as analyzed by Western blot (see Fig. 8, right panel). Representative blots are depicted (lane 1, controls and lane 2, glycerol treatment samples).

In vivo mouse experiments: Endotoxemic ARF

FATP2 protein and mRNA analyses. As shown in Figure 9, left panel, by 18 hours post-LPS injection, an approximate 25% reduction in renal cortical FATP2 protein was observed (representative blots are depicted) (Fig. 9, left panel, lane 1, controls and lane 2, LPS treatment). This was not matched by a reduction in FATP1 mRNA. Rather a slight, but significant, increase in FATP mRNA was apparent at 18 hours post-LPS administration (Fig. 9, right panel). LPS injection severely compromised renal function, as denoted by 18-hour BUN analysis (controls 29 ± 2 mg/dL vs. 96 ± 4 mg/dL) ($P < 0.0001$).

DGAT1 and DAGT2 mRNA levels after LPS-induced ARF. As shown in Figure 10, left panel, DGAT1 and DGAT2 mRNAs were increased by ~65% and ~45%,

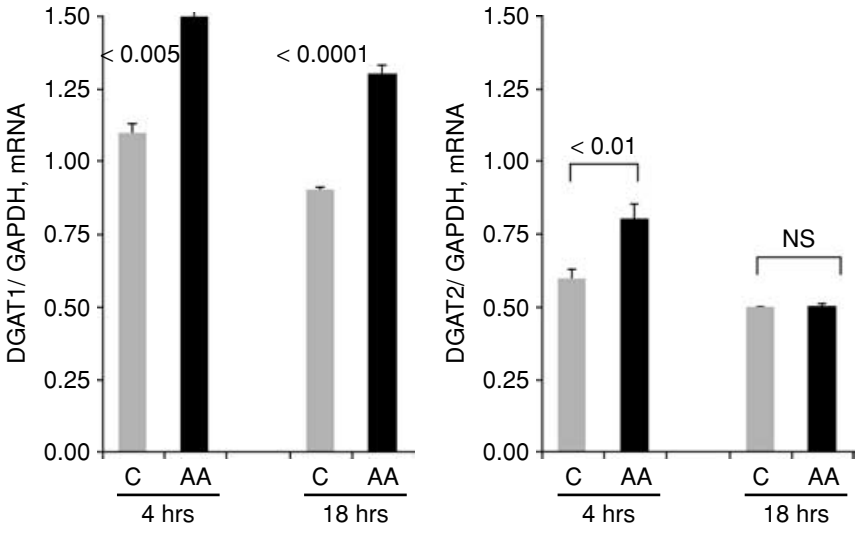

Fig. 4. Acyl-coenzyme A:diacylglycerol acyltransferases DGAT1 and DGAT2 mRNA responses to antimycin A–mediated human kidney 2 (HK-2) cell injury. Left panel, Antimycin A induced significant elevations in DGAT1 mRNA levels after both 4-hour and 18-hour incubations. Right panel, DGAT2 mRNA levels were also increased by antimycin A exposure, but the effect was transient, with a significant difference being observed after 4, but not 18 hours, of antimycin A treatment.

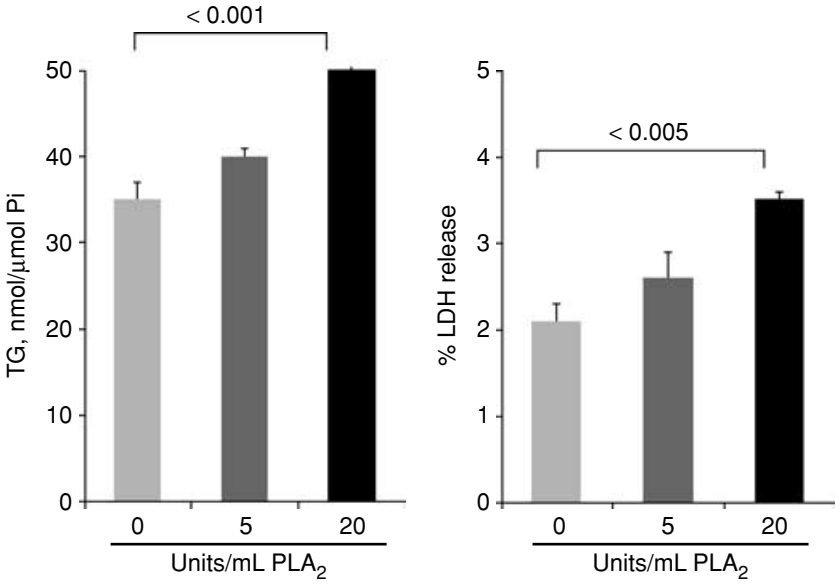

Fig. 5. Exogenous phospholipase A_2 (PLA_2) effects on human kidney 2 (HK-2) cell triglyceride (TG) content. Left panel, Pancreatic PLA_2 addition to HK-2 cells caused a dose dependent increase in triglyceride content. Right panel, This PLA_2 effect occurred despite minimal lethal cell injury, as assessed by% lactate dehydrogenase (LDH) release (increases of ≤2% even at the 20 U/mL dosage).

respectively, by 18 hours post-LPS treatment. This corresponded to a previously observed three- to fourfold increase in triglyceride levels at this time point [13].

FAS protein expression following endotoxemia. FAS protein levels appeared to be unaffected by the endotoxemic state, as assessed by Western blot analysis. Values and representative blots are presented in Figure 10, right panel (control, lane 1 and LPS treatment, lane 2).

Tissue lipase activity with the in vitro and in vivo injury protocols

Both the post-glycerol and post-ischemic renal cortical tissues had significant depressions in tissue lipase activity (Fig. 11). Conversely, in the case of endotoxemia, a significant increase in lipase activity was discerned [Note: pilot data indicated that differences in tissue lipase did not result from differences in plasma lipase levels, with possible contamination of tissue samples, as plasma lipase levels were assayed with a commercially available kit (#805B) (Trinity Biotech; Jamestown, NY) and values were highly comparable for the controls vs. the experimental groups].

DISCUSSION

In a previous study [13], we demonstrated that increased extracellular fatty acid uptake, with subsequent conversion into triglyceride, is one mechanism by which cell injury can evoke a triglyceride loading state. This statement was based on the observation that when fatty acids were added to antimycin A–challenged HK-2 cells, exaggerated triglyceride formation resulted. One potential mediator of increased fatty acid uptake, with subsequent triglyceride formation, would be an injury-induced

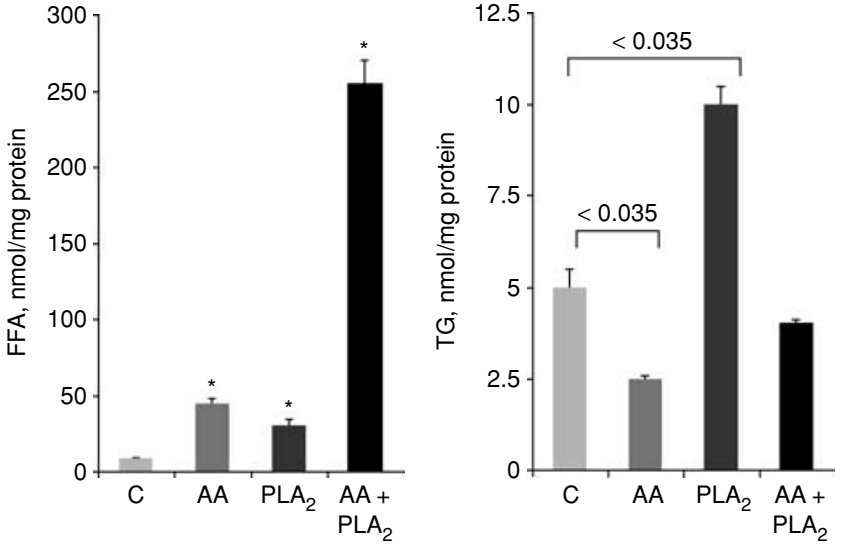

Fig. 6. Antimycin A (AA) effects on mouse isolated proximal tubule free fatty acid (FFA) and triglyceride (TG) content. Left panel, Both antimycin A and exogenous phospholipase A_2 (PLA_2) addition to isolated mouse proximal tubules caused modest increases in FFA content ($^*P < 0.05$). When antimycin A and PLA_2 were added together, a striking synergistic increase in FFA accumulation resulted. Right panel, Despite the fact that antimycin A could increase FFA (i.e., triglyceride substrate) content, when added by itself to proximal tubules, antimycin A suppressed triglyceride levels by ~50%. Conversely, PLA_2 addition to isolated tubules caused an approximate doubling of triglyceride content. However, this PLA_2-induced triglyceride increase was completely blocked by concomitant antimycin A treatment. Thus, these results are consistent with the concepts that (*1*) mitochondrial inhibition raises FFA levels (due to decreased mitochondrial consumption ± endogenous PLA_2 activation); and (*2*) if adenosine triphosphate (ATP) depletion results (as is the case with antimycin A treatment of isolated tubules), the liberated FFAs cannot be incorporated into cellular triglyceride pools (presumably because of a failure of fatty acid activation).

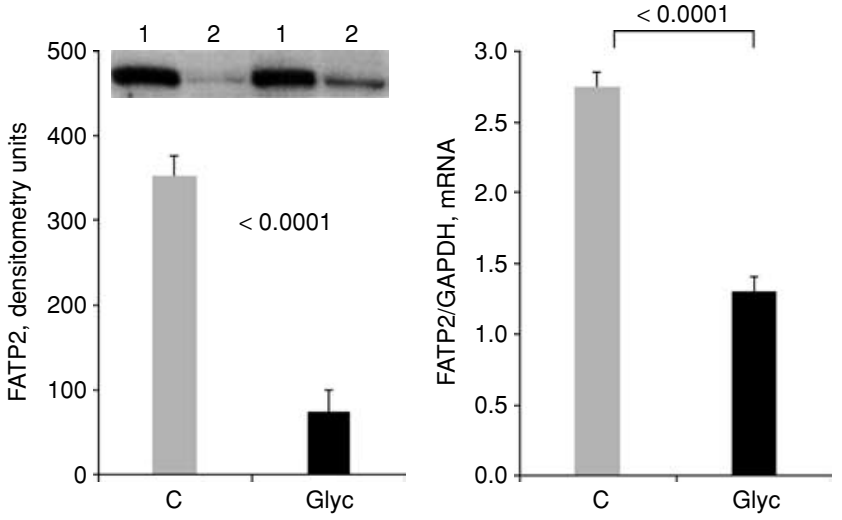

Fig. 7. Glycerol-induced acute renal failure (ARF): Effects on fatty acid transport protein 2 (FATP2) protein/mRNA expression. Left panel, By 18 hours post-glycerol (glyc) injection, an approximate 80% reduction in FATP2 protein levels was observed, compared to values observed in control (C) kidneys. Representative blots (lane 1, controls and lane 2, glycerol treatment) are depicted. Right panel, The reduction in FATP2 protein was accompanied by a comparable decrement in FATP2 mRNA, suggesting that FATP2 reductions may have been, in part, due to decreased gene transcription/message translation.

increase in FATP2, the dominant renal tubular plasma membrane fatty acid transporter [25, 26]. The present study provides direct support for this hypothesis. When antimycin A–treated HK-2 cells were probed for FATP2, an approximate twofold increase was noted by Western blot. A comparable increase in FATP2 mRNA accompanied the protein increase, suggesting that increased transcription was at least partially responsible. To our knowledge, this is the first demonstration that FATP2, and its message, can be induced by an acute tubular cell injury state.

While our findings indicate that antimycin A–induced injury can increase FATP2 levels, potentially increasing fatty acid uptake [13], the present HK-2 cell studies also illustrate that HK-2 cells can accumulate triglyceride independently of FATP2-mediated fatty acid transport. This conclusion is based on the fact that the employed HK-2 cell culture medium (K-SFM) has no free fatty acid content (confirmed by medium fatty acid assay, both before and after the antimycin A challenge; pilot data). The absence of exogenous fatty acid precludes increased extracellular fatty acid uptake; nevertheless, antimycin A still doubled HK-2 cell triglyceride content (Fig. 2). Thus, alternative mechanisms for triglyceride accumulation must exist. This led us to explore the possibility that injury might increase FAS, providing de novo fatty acid for DGAT-mediated triglyceride formation. Western blot analysis confirmed that antimycin A treatment

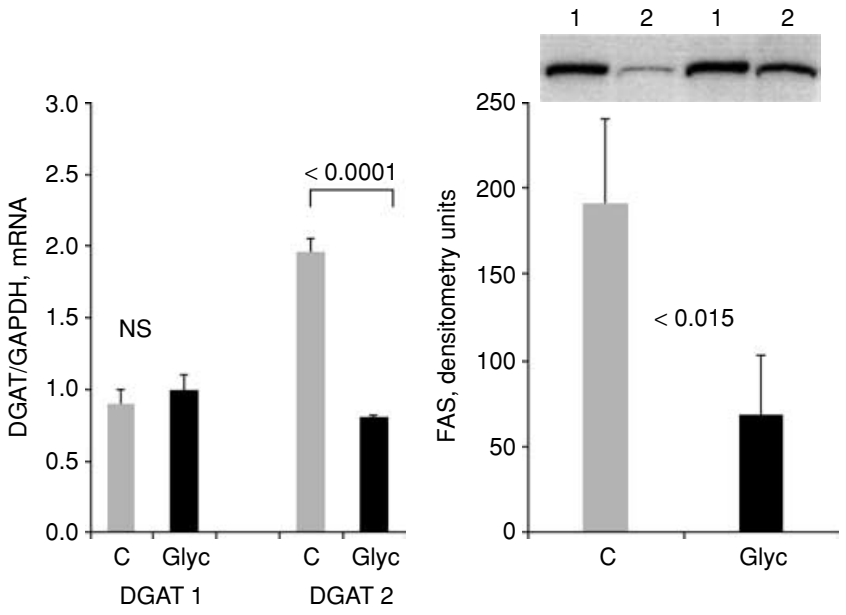

Fig. 8. Glycerol-induced acute renal failure (ARF): Effects on acyl-coenzyme A:diacylglycerol acyltransferase DGAT mRNAs and fatty acid synthase (FAS) expression. Left panel, DGAT1 and DGAT2 mRNAs were assessed 18 hours post-glycerol (glyc) injection. DGAT1 message remained unchanged. However, an approximate 50% reduction in DGAT2 mRNA was observed. Right panel, FAS expression was reduced by ~50% following glycerol injection, suggesting that de novo fatty acid synthesis is an unlikely explanation for the glycerol-induced triglyceride increments [13].

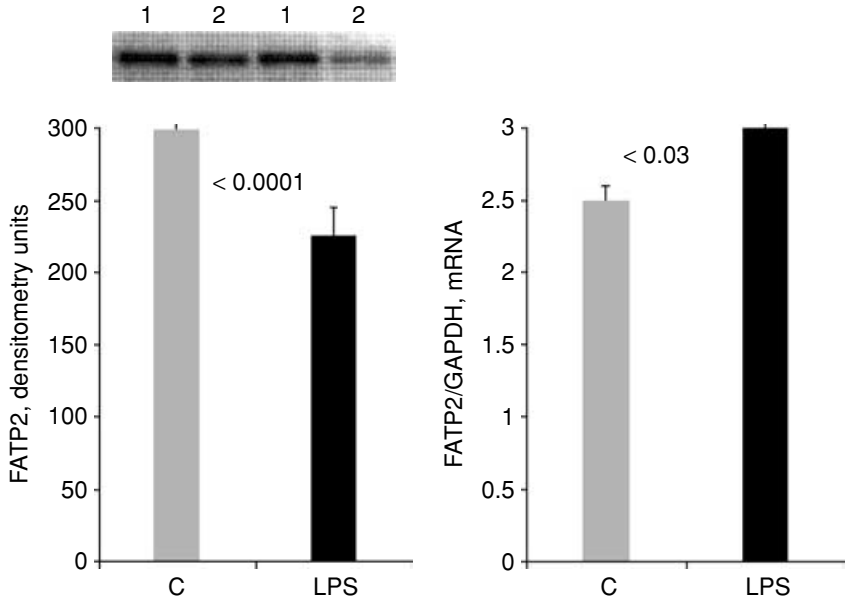

Fig. 9. Lipopolysaccharide (LPS)-induced acute renal failure (ARF): Effects on fatty acid transport protein 2 (FATP2) protein/mRNA expression. Left panel, LPS caused a modest, but significant, reduction in FATP2 protein levels. Right panel, FATP2 mRNA values were increased, rather than suppressed, at the time of the FATP2 protein reduction.

can, indeed, increase FAS levels. This suggested that de novo fatty acid synthesis might be critical to antimycin A–mediated triglyceride accumulation. However, the results obtained with cerulenin rule out this hypothesis, given that this FAS inhibitor did not prevent triglyceride loading during antimycin A–induced HK-2 cell attack. Of note, cerulenin lowered HK-2 cell triglyceride levels by ~75% in the absence of antimycin A. This confirmed its ability to inhibit HK-2 cell FAS. Thus, the data derived from the above two sets of experiments indicate that although increased FATP2-mediated fatty acid transport and increased FAS expression might each contribute to antimycin A–mediated triglyceride loading, additional mechanisms for the triglyceride pool enhancement must exist.

Given the above, we tested a third hypothesis: that antimycin A, which is known to activate PLA_2 in cultured tubular cells, releasing FFAs from phospholipids [27], might allow for DGAT-mediated fatty acid flux into triglyceride pools. To test this hypothesis, HK-2 cells were incubated with exogenous PLA_2, followed by triglyceride assessment. Indeed, PLA_2 induced dose-dependent triglyceride formation, directly supporting the above hypothesis. To ascertain whether antimycin A might also stimulate DGAT expression, DGAT1 and DGAT2 mRNAs were assessed, and increases in both were observed.

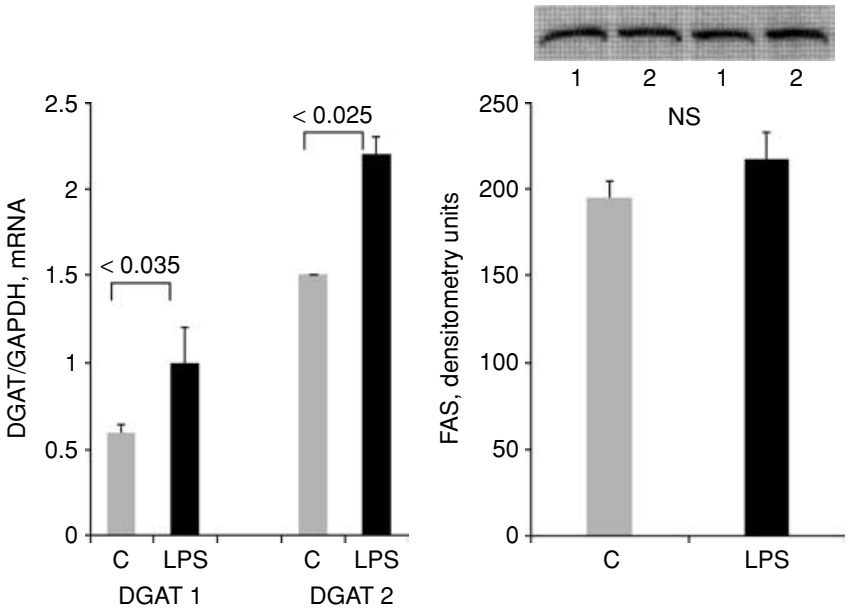

Fig. 10. Lipopolysaccharide (LPS)-induced acute renal failure (ARF): Effects on acyl-coenzyme A:diacylglycerol acyltransferase DGAT message and fatty acid synthase (FAS) expression. Left panel, Renal cortical DGAT1 and DGAT2 mRNAs were assessed 18 hours post-LPS injection. At the 18-hour time point, both message levels were significantly increased, compared to controls. Right panel, No significant change in FAS levels were apparent in post-LPS treated kidneys, as assessed by Western blotting (lane 1, control and lane 2, post-LPS).

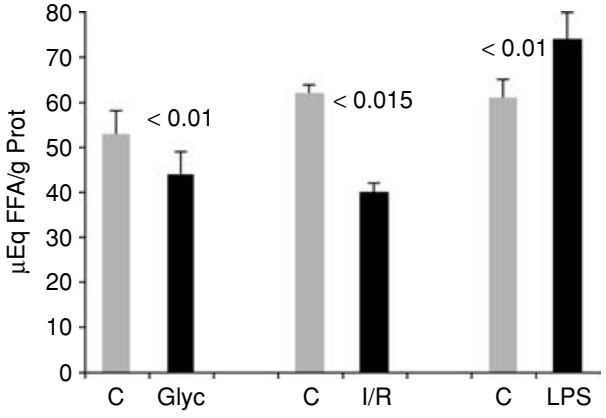

Fig. 11. Tissue lipase activity 18 hours post in vivo renal injury protocols. Glycerol-induced renal injury (Glyc), and ischemic/reperfusion (I/R) injury each caused signficant reductions in renal cortical lipase activity (~20% and ~35%, respectively), compared to their controls (C). Conversely, by 18 hours post-LPS injection, a significant increase in renal cortical lipase levels was apparent.

We were unable to ascertain whether these mRNA increments up-regulate DGAT protein, due to a lack of available antibodies for Western blotting. Nevertheless, the mRNA results do suggest that antimycin A provides the appropriate stimulus for such a result.

A number of theoretic links exist between mitochondrial respiration, FFA availability, and triglyceride formation. Given that the mitochondrion utilizes fatty acids for ATP production via beta oxidation, decreased mitochondrial respiration would be expected to decrease fatty acid consumption, potentially increasing FFA availability for triglyceride synthesis. Conversely, if severe ATP depletion results, ATP dependent "activation" of accumulating fatty acids (via acyl-coenzyme A formation) might cease, possibly preventing FFA incorporation into triglyceride pools (see Fig. 1). To evaluate these possibilities, the impact of mitochondrial blockade on FFA levels and triglyceride formation was assessed. Freshly isolated mouse proximal tubules were used for this purpose, given that they (unlike HK-2 cells) [33] are completely dependent on aerobic ATP production. Antimycin A markedly increased proximal tubule FFA levels, particularly, when exogenous PLA_2 was present (Fig. 5). This is consistent with the concept that mitochondrial blockade can decrease FFA consumption, potentially raising FFA pools. Also noteworthy was the finding that antimycin A–induced mitochondrial blockade inhibited proximal tubule triglyceride formation, despite the FFA increases. For example, whereas PLA_2 treatment doubled tubule triglyceride levels in the absence of antimycin A, PLA_2 failed to increase triglycerides when antimycin A was present. Furthermore, antimycin A decreased, rather than increased, triglyceride levels in non-PLA_2-exposed tubules. These results underscore two relevant points. First, decreased mitochondrial respiration can increase FFA levels. Second, despite this result, if profound ATP depletion results, the accumulated FFAs cannot be converted into cellular triglyceride pools (presumably due to lack of ATP-dependent fatty acid activation). Given these findings, it seems clear that no simple, direct relationship exists between mitochondrial respiration, FFA increments, and corresponding triglyceride levels. Of note, when antimycin A is added to HK-2 cells, mitochondrial blockade, but only mild ATP reductions, develops (due to continued anaerobic ATP production) [33]. Thus, under these circumstances, mitochondrial blockade, with decreased mitochondrial fatty acid consumption, might well enhance triglyceride pools.

Table 3. Summary of results and comparisons of injury models

	FATP2 (protein)	FATP2 (mRNA)	FAS (protein)	DGAT1 (mRNA)	DGAT2 (mRNA)	Lipase
HK-2: AA	↑	↑	↑	↑	↑	ND
Glycerol	↓	↓	↓	NS	↓	↓
Endotoxin	↓	↑	NS	↑	↑	↑

Abbreviations are: FATP2, fatty acid transport protein 2; FAS, fatty acid synthase; DGAT, acyl-coenzyme A:diacylglycerol acyltransferase; HK-2 human kidney 2; AA, antimycin A, NS, no significant change; ND, not done.

The directional results for the assessments which were made are presented. Lipase activity could not be accurately assessed in the HK-2 cell experiments due to insufficient assay sensitivity. Thus, in addition to assessing lipase activity in the glycerol and endotoxemic model, a third in vivo model, in vivo ischemia/reperfusion, was undertaken and the results are presented in Figure 11.

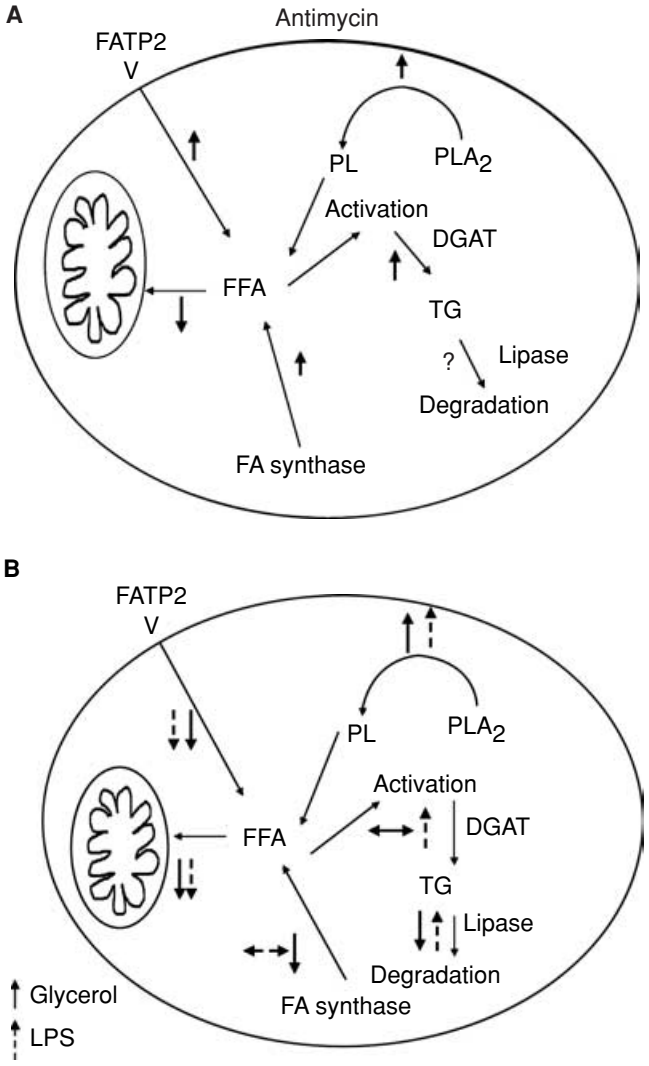

Fig. 12. (*A*) Proposed pathways of triglyceride (TG) accumulation in human kidney 2 (HK-2) cells with antimycin A. The data gathered suggest that essentially all of the proposed pathways in cellular triglyceride homeostasis are perturbed during antimycin A–mediated HK-2 cell injury, each favoring increased triglyceride levels. These include (*1*) upregulation of fatty acid transport protein 2 (FATP2) expression (protein and mRNA), augmenting fatty acid uptake (assuming the presence of extracellular fatty acids); (*2*) increased phospholipase A_2 (PLA_2) activity [27] would also lead to increased triglyceride formation [via fatty acid mobilization from phospholipids (PL)]; (*3*) increased fatty acid (FA) synthase (FAS), which could contribute to triglyceride formation; (*4*) antimycin A–induced mitochondrial blockade, decreasing fatty acid consumption (thereby increasing fatty acid pools); and (*5*) increased acyl-coenzyme A:diacylglycerol acyltransferases DGAT mRNA expression, presumably increasing DGAT enzyme expression/activity, and hence, triglyceride synthesis (lipase activity in antimycin A–challenged HK-2 cells could not be ascertained). **(*B*) Potential pathways involved with triglyceride homeostasis with in vivo renal injury**. The solid and dashed arrows represent the glycerol and the lipopolysaccharide (LPS) models of acute renal failure (ARF), respectively. ↑, ↓, and ← → represent increased, decreased, or unchanged activities, respectively. Unlike, the HK-2 model, FATP2 protein expression was suppressed by both glycerol and LPS-mediated renal injury. This observation, plus the fact that FAS failed to increase with either in vivo injury model, suggest that PLA_2 activation/PL degradation (known to occur with both forms of injury), coupled with decreased mitochondrial fatty acid consumption [dictated either by mitochondrial injury or a decrease in glomerular filtration rate (GFR)], are the dominant factors providing excess fatty acid for triglyceride synthesis. The latter can occur whether or not DGAT mRNA levels are increased. Finally, tissue lipase activity is an additional arbitor of triglyceride levels in these two injury models, given that it can either fall (glycerol) or rise (LPS) with in vivo renal damage.

In addition to increased triglyceride formation, impacted by the multiple factors discussed above, decreased triglyceride hydrolysis could also contribute to a triglyceride loading state. We were unable to ascertain the impact of antimycin A on HK-2 cell lipase levels, due to a relative lack of sensitivity of the developed assay. However, to gain insights into this issue, tissue lipase activity was assessed following three forms of in vivo injury: I/R, glycerol induced rhabdomyolysis, and endotoxemic ARF. Noteworthy were the findings that both I/R and glycerol-induced rhabdomyolysis caused 20% to 35% reductions in renal cortical lipase activity. Thus, increased triglyceride synthesis may not be the sole explanation for a post-injury triglyceride loading state. However, it is also noteworthy that in the case of endotoxemia, increased, not decreased, lipase activity resulted. The reason for this striking difference in lipase activity amongst these three in vivo injury models remains unknown. However, given the marked differences between endotoxemia, a hemodynamic form of ARF, vs. I/R or glycerol-induced acute tubular necrosis, differences in lipase activity should not be unexpected. These differences underscore that triglyceride accumulation in post-injured tissues can arise from multiple, complex, and likely disease-specific perturbations in triglyceride homeostatic pathways.

To further contrast mechanisms for injury-evoked triglyceride accumulation, triglyceride synthetic pathways during the glycerol and endotoxemic models of

ARF were assessed. The results obtained were then contrasted both between these two injury models, and with the previously obtained in vitro HK-2 cell results. Indeed, striking differences among these injury models were observed, which are outlined in Table 3. Most notable were the following: (*1*) in contrast to heightened FATP2 expression in antimycin A–challenged HK-2 cells, FATP2 protein levels were markedly suppressed with in vivo ARF (particularly following rhabdomyolysis); (*2*) whereas FAS was elevated following antimycin A–induced HK-2 cell injury, it was either suppressed (glycerol) or unchanged (LPS) following in vivo ARF; and (*3*) antimycin A augmented HK-2 cell DGAT mRNAs; conversely, DGAT messages were either increased (LPS), or decreased (glycerol) following in vivo ARF. These differences, once again, underscore that multiple and disease specific pathways likely contribute to a post-injury triglyceride loading state. Based on the information gathered above, the dominant pathways thought to contribute to triglyceride accumulation in each of the models studied are presented schematically in Figure 12.

CONCLUSION

The present experiments have evaluated potential mechanisms of cellular triglyceride accumulation following highly divergent in vivo and in vitro models of tubular cell damage. The data obtained underscore the complexity of this process, which may involve alterations in triglyceride synthesis (DGAT expression), fatty acid (triglyceride substrate) availability (FATP2, FAS, PLA_2 activity, and mitochondrial FFA consumption), and triglyceride degradative (lipase) pathways. The degrees to which each of these may participate in injury-induced triglyceride accumulation appear to vary greatly, depending on the types of tissue injury sustained. Thus, the concept that injury-induced triglyceride accumulation simply stems from a flux of excess fatty acid into triglyceride pools would seem to underestimate the complexity of the issues at hand. That triglyceride accumulation expresses itself despite divergent underlying mechanisms would seem to underscore the importance of this process to cellular homeostasis in the aftermath of diverse forms tubular cell attack.

ACKNOWLEDGMENTS

The authors thank Ms. SY Hanson and Mr. Steven Lund, Fred Hutchinson Cancer Center, Seattle, WA for their expert technical assistance. This work was supported by research grants from the National Institutes of Health (R01 DK68520-01; R37 DK038432-17; and RO1 DK066336), and by a Career Development Award (to A.S.) from the American Diabetes Association (7-04-CD-14).

Reprint requests to Richard A. Zager, Fred Hutchinson Cancer Research Center 1100 Fairview Ave. N; Room D2-190 Seattle, WA 98109. E-mail: dzager@fhcrc.org

REFERENCES

1. Meegalla RL, Billheimer JT, Cheng D: Concerted elevation of acyl-coenzyme A:diacylglycerol acyltransferase (DGAT) activity through independent stimulation of mRNA expression of DGAT1 and DGAT2 by carbohydrate and insulin. *Biochem Biophys Res Commun* 298:317–323, 2002
2. McGarry JD, Kuwajima M, Newgard CB, *et al*: From dietary glucose to liver glycogen: The full circle round. *Annu Rev Nutr* 7:51–73, 1987
3. Janssen U, Stoffel W: Disruption of mitochondrial beta—Oxidation of unsaturated fatty acids in the 3,2-trans-enoyl-CoA isomerase-deficient mouse. *J Biol Chem* 277:19579–19584, 2002
4. Listenberger LL, Han X, Lewis SE, *et al*: Triglyceride accumulation protects against fatty acid-induced lipotoxicity. *Proc Natl Acad Sci USA* 100:3077–3082, 2003
5. Schaeffer JE: Lipotoxicity: When tissue overeat. *Curr Opin Lipidology* 14:281–287, 2003
6. Feldstein AE, Werneburg NW, Canbay A, *et al*: Free fatty acids promote hepatic lipotoxicity by stimulating TNF-alpha expression via a lysosomal pathway. *Hepatology* 40:185–194, 2004
7. Matthys E, Patel Y, Kreisberg J, *et al*: Lipid alterations induced by renal ischemia: Pathogenic factor in membrane damage. *Kidney Int* 26:153–161, 1984
8. Zager RA, Iwata M, Conrad DS, *et al*: Altered ceramide and sphingosine expression during the induction phase of ischemic acute renal failure. *Kidney Int* 52:60–70, 1997
9. Zager RA, Conrad DS, Burkhart K: Phospholipase A_2: A potentially important determinant of adenosine triphosphate levels during hypoxic-reoxygenation tubular injury. *J Am Soc Nephrol* 7:2327–2339, 1996
10. Cases S, Smith SJ, Zheng YW, *et al*: Identification of a gene encoding an acyl CoA:diacylglycerol acyltransferase, a key enzyme in triacylglycerol synthesis. *Proc Nat Acad Sci USA* 95:13018–13023, 1998
11. Kao Y, Manzon RG, Sheridan MA, Youson JH: Study of the relationship between thyroid hormones and lipid metabolism during $KClO_4$-induced metamorphosis of landlocked lamprey, Petromyzon marinus. *Comp Biochem Physiol Part C Pharmacol Toxicol Endocrinol* 122:363–373, 1999
12. Tannenbaum J, Purkerson ML, Klahr S: Effect of unilateral ureteral obstruction on metabolism of renal lipids in the rat. *Am J Physiol* 245: F254–F262, 1983
13. Zager RA, Johnson ACM, Hanson SY: Renal tubular triglyceride accumulation following endotoxic, toxic, and ischemic injury. *Kidney Int* (in press)
14. Brindley DN: Metabolism of triacylglycerols, in *Biochemistry of Lipids, Lipoproteins, and Membranes*, edited byVance DE, Vance JE, Amsterdam, Elsevier 1991, pp 171–203
15. Lehner R, Kuksis A: Biosynthesis of triacylglycerols. *Prog Lipid Res* 35:169–201, 1996
16. Farese RV Jr., Cases S, Smith SJ: Triglyceride synthesis: Insights from the cloning of diacylglyerol acyltransferase. *Curr Opin Lipidol* 11: 229–234, 2000
17. Ryan MJ, Johnson G, Kirk J, *et al*: HK-2: an immortalized proximal tubule epithelial cell line from normal adult human kidney. *Kidney Int* 45:48–57, 1994
18. Johnson AC, Yabu JM, Hanson S, *et al*: Experimental glomerulopathy alters renal cortical cholesterol, SR-B1, ABCA1, and HMG CoA reductase expression. *Am J Pathol* 162:283–291, 2003
19. Zager RA, Shah VO, Shah HV, *et al*: The mevalonate pathway during acute tubular injury: Selected determinants and consequences. *Am J Pathol* 161:681–692, 2002
20. VanVeldhoven PP, Mannaerts GP: Inorganic and organic phosphate measurements in the nanomolar range. *Anal Biochem* 161:45–48, 1987
21. Menendez JA, Vellon L, Mehmi I, *et al*: Inhibition of fatty acid synthase (FAS) suppresses HER2/neu (erbB-2) oncogene overexpression in cancer cells. *Proc Natl Acad of Sci USA* 101:10715–10720, 2004
22. Yasuno R, von Wettstein-Knowles P, Wada H: Identification and molecular characterization of the beta-ketoacyl-[acyl carrier

protein] synthase component of the Arabidopsis mitochondrial fatty acid synthase. *J Biol Chem* 279:8242–8251, 2004
23. Chirala SS, Huang WY, Jayakumar A, *et al*: Animal fatty acid synthase: Functional mapping and cloning and expression of the domain I constituent activities. *Proc Natl Acad Sci USA* 94:5588–5593, 1997
24. Jayakumar A, Tai MH, Huang WY, *et al*: Human fatty acid synthase: Properties and molecular cloning. *Proc Natl Acad Sci USA* 92:8695–8699, 1995
25. Stahl A, Gimeno RE, Tartaglia LA, Lodish HF: Fatty acid transport proteins: A current view of a growing family. *Trends Endocrinol Metab* 12:266–273, 2001
26. Stahl A: A current review of fatty acid transport proteins (SLC27). *Pflugers Archiv Eur J Physiol* 447:722–727, 2004
27. Venkatachalam MA, Patel YJ, Kreisberg JL, Weinberg JM: Energy thresholds that determine membrane integrity and injury in a renal epithelial cell line (LLC-PK_1). *J Clin Invest* 81:745–758, 1988
28. Kalhorn T, Zager RA: Renal cortical ceramide patterns during ischemic and toxic injury: Assessments by HPLC-mass spectrometry. *Am J Physiol* 277:F723–733, 1999
29. Zager RA, Mahan J, Merola AJ: Effects of mannitol on the postischemic kidney: Biochemical, functional, and morphologic assessments. *Lab Invest* 53: 433–442, 1985
30. Nath KA, Grande JP, Croatt AJ, *et al*: Intracellular targets in heme protein-induced renal injury. *Kidney Int* 53:100–111, 1998
31. Feldkamp T, Kribben A, Roeser NF, *et al*: Preservation of complex I function during hypoxia-reoxygenation-induced mitochondrial injury in proximal tubules. *Am J Physiol* 286:F749–F759, 2004
32. Zager RA, Burkhart KM: Differential effects of glutathione and cysteine on Fe^{2+}, Fe^{3+}, H_2O_2 and myoglobin-induced proximal tubular cell attack. *Kidney Int* 53:1661–1672, 1998
33. Iwata M, Herrington J, Zager RA: Protein synthesis inhibition induces cytoresistance in cultured human proximal tubular (HK-2) cells. *Am J Physiol* 268:F1154–F1163, 1995
34. Weinberg JM, Davis JA, Abarzua M, Rajan T: Cytoprotective effects of glycine and glutathione against hypoxic injury to renal tubules. *J Clin Invest* 80:1446–1454, 1987
35. Zager RA, Burkhart KM, Conrad DS, *et al*: Phospholipase A_2-induced cytoprotection of proximal tubules: potential determinants and specificity for ATP depletion-mediated injury. *J Am Soc Nephrol* 7:64–72, 1996
36. Zager RA, Iwata M, Burkhart KM, Schimpf BA: Post-ischemic acute renal failure protects proximal tubules from O_2 deprivation injury, possibly by inducing uremia. *Kidney Int* 45:1760–1768, 1994